Mode-splitting in a ring resonator for self-referenced sensing

(Student paper)

M. de Goede[1], M. Dijkstra[1], N. Acharyya[2,3], G. Kozyreff[2] and S.M. García-Blanco[1]
[1] Optical Sciences, MESA+ Institute for Nanotechnology, University of Twente, P.O. Box 217, 7500 AE Enschede, the Netherlands
[2] Optique Nonlinéaire Théorique, Université libre de Bruxelles, CP 231, Brussels, Belgium
[3] Max-Born-Institut für Nicthlineare Optik und Kurzzeitspektroskopie, D-12489 Berlin, Germany
e-mail: m.degoede@utwente.nl

ABSTRACT

An optical microring resonator has a two-fold degeneracy corresponding with two counterpropagating modes, one travelling in the clockwise and the other in the counterclockwise direction. Inserting a Bragg grating on the surface of the ring provides coupling between these modes, which lifts the degeneracy and induces mode-splitting of the resonances. The amount of mode-splitting is directly related to the reflectivity of the grating and can be affected by structurally modifying the grating by, for instance, binding of biomolecules to it. Environmental perturbations to the surroundings of the grating, such as temperature or bulk refractive index variations, hardly affect the grating reflectivity, and thus the mode-splitting. This principle allows self-referenced sensor operation based on variations of the mode-splitting induced by structural changes of the grating.

Keywords: microring resonator, mode-splitting, biosensing, Al_2O_3

1. INTRODUCTION

A strong demand exists for simple-to-use, label-free, portable, sensitive sensing systems that can be used for the detection of biomolecules for healthcare applications [1]. Optical ring resonators are excellent candidates to this goal [2]. Optical ring resonator sensors usually work by monitoring a shift of their resonance wavelength due to particle binding events, which elongate the optical path of the ring resonator. Another approach is based on the splitting of their resonance modes. Optical resonators support two degenerate modes sharing the same resonance wavelength traveling in the counterpropagation clockwise (CW) and counterclockwise (CCW) directions. The binding of a scattering medium to the resonator provides mutual coupling between the CW and CCW modes, lifting their degeneracy resulting in a doublet splitting of the original resonant wavelength [3], as shown in Figure 1. Using this transducing scheme, individual binding events of nanoparticles and even single viruses have been detected [4]. Since the variations of the mode splitting are due to the magnitude of the scattering, these sensors are to first-order insensitive to environmental variations such as temperature fluctuations or variations in bulk refractive index [5]. In this paper, the first experimental demonstration of a biosensor based on mode-splitting is presented. A Bragg reflector grating made of poly(methyl methacrylate) (PMMA) was nanofabricated on the surface of an aluminum oxide (Al_2O_3) ring resonator [6]. The Al_2O_3 surface was selectively functionalized to bind antibodies to selectively capture the rhS100A4 protein [6]. This protein has been selected because it is related to human tumor development [7].

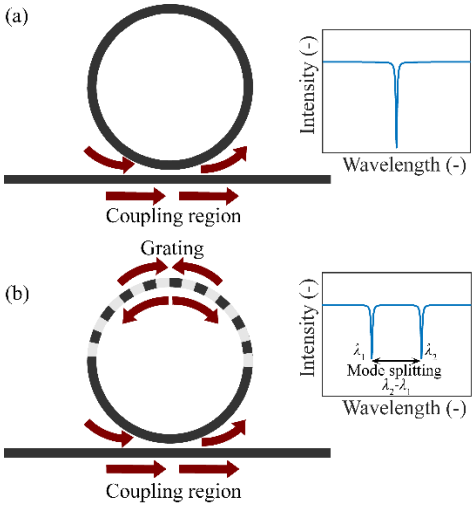

Figure 1. Microring resonator mode-splitting. (a) Pristine microring resonator. Inset shows degenerate resonance. (b) Microring resonator with grating. Inset shows resonance mode-splitting.

2. GRATING FABRICATION

An Al_2O_3 dielectric layer was reactively sputter deposited on a thermally oxidized silicon substrate (oxide thickness of 8 µm), following the process described in [8]. The substrate temperature was set to 450ºC. An RF power of 200 W was applied to an Al target. Gas flows of 2.5 sccm of reactive oxygen inside the chamber and 30 sccm of argon applied to the Al target were employed, resulting in a process chamber pressure of 3.7 mTorr. The bus and microring resonator waveguides were then patterned using contact lithography (Olin OIR 906-12 photoresist and EVG 620 exposure tool) and subsequently etched with a reactive ion plasma of BCl_3 and HBr at a ratio of 5:2 and a total power of 25 W (Oxford Plasmalab System 100) [9]. Device parameters were a ring radius of 150 µm, coupling gap of 0.8 µm and waveguide cross section of 0.8×2.4 µm^2. A PECVD SiO_2 cladding 3 µm thick was deposited (Oxford Plasmalab 80 Plus, deposition temperature of 300 ºC) using a shadow mask such that the ring resonator remains exposed to the environment, while burying the input and output bus waveguides and end facets. The wafer was then diced into small chips and cleaned with HNO_3 and deionized water.

A PMMA Bragg grating was printed over the device using electron beam lithography. This method has a simple fabrication process requiring only the patterning and development of the grating, without any subsequent deposition or processing steps. First, a PMMA layer (NANO™ 950PMMA A4) was spun at 4 krpm for 1 minute to achieve a thickness of ~25 nm on top of the waveguide. Then, a chromium coating ~5 nm thick was sputter coated at a power of 200 W and base pressure of 6.6×10^{-3} mBar. This layer prevents charging during the electron beam exposure. Then, the grating pattern is exposed on top of the resist with a RAITH150 Two electron beam lithography tool. A dose of 180 µC/cm^2 was used, together with an acceleration voltage of 10 kV. The fabricated grating parameters were a period of 535 nm, a length of the grating of 4/5 of the circumference of the ring and a fill fraction of 0.35 (on the mask). After exposure and patterning, the Cr layer was removed by wet etch with a mixture of perchloric acid and ceric ammonium nitrate (TechniEtch Cr01) for 10 seconds, followed by a rinse in deionized water. The exposed PMMA is subsequently developed with a mixture of MIBK:IPA at a ratio 1:3 for 40 seconds, after which the device is rinsed with IPA for 20 seconds and blown dry with N_2. The resulting PMMA grating has a fill factor of ~0.5. Finally, a PDMS channel with dimensions of 600 µm width and 70 µm height was bonded onto the chip and connected to a syringe pump to submerge the microring resonator in deionized water.

3. RESULTS

To optically characterize the device, its transmission spectrum was continuously recorded using an Agilent 81646 tunable laser at a wavelength of 1625 nm. TE-polarized laser light was guided through single mode polarization maintaining fibers (PM1500-XP) and coupled to the sample. Before grating fabrication, the spectrum of the ring resonator contains multiple degenerate resonances. After fabrication of the grating, mode-splitting of the resonance modes is clearly observed. The measured maximum mode-splitting lies around a wavelength of 1627 nm and amounts to ~298 pm.

The device was then used to demonstrate biosensing by modifying its mode-splitting through binding of biomolecules to alter the reflectivity of the grating. Figure 2 (a) illustrates the three-step protocol to deposit the biomolecules inside the grating teeth was developed. First, the sample and 200 µl of (3-Glycidyloxypropyl)trimethoxysilane (GPTMS, Sigma Aldrich 440167) are placed in a desiccator for 4 hours to apply a silane functionalization through evaporation. After applying the functionalization protocol, the device was exposed to a flow of 10 mM phosphate buffer saline (PBS) in order to establish a baseline. The amount of initial mode splitting was 297.6 pm. A solution of anti-S100A4 antibody at a concentration of 200 µg/ml in 10 mM PBS was prepared and flown over the device. Upon flowing the antibodies over the device, antibodies bonded to the grating, resulting in a reduction of the mode-splitting. In this case, the mode-splitting is lowered from 297.6 to 288.4 pm. This is followed by a flow of the rhS100A4 proteins at concentrations of both 1 and 5 µM in 10 mM PBS. Mode-splitting variations of ~4 and ~6 pm respectively were measured.

The changes of the mode-splitting are rather small compared to the resonance wavelength shifts encountered in conventional ring resonator sensing. This is because the mode-splitting does not measure changes of the effective index of the mode travelling inside the ring, but changes of the grating reflectivity due to the presence of the biomolecules. Since these molecules are rather small with a low refractive index of ~1.5 [10], the effect on the grating is expected to be low. Furthermore, some of the antibodies and biomarkers can still bind to Al_2O_3 and PMMA through adsorption, lowering the relative change due to grating reflectivity modification. This type of sensor can perform better when one uses larger target analytes, such as cancer biomarker extracellular vesicles [11], nanoparticles, bacteria or denser materials with a higher refractive index. One might also monitor the mode-splitting at a wavelength at the edge of the reflectivity spectrum instead of at the Bragg wavelength, where the reflectivity profile is relatively flat. Then, a shift of both the resonance and Bragg wavelength results in the mode experiencing another reflectivity, which is accompanied by a change in mode-splitting [12]. Despite this scheme having an increased sensitivity, its self-referenced nature is cancelled. On the other hand, by covering the whole ring with a grating but functionalizing it only over a quarter of the perimeter, most of the splitting can be

concentrated on a single resonance [13]. In this way, self-referencing can be preserved while raising the sensitivity to standard values.

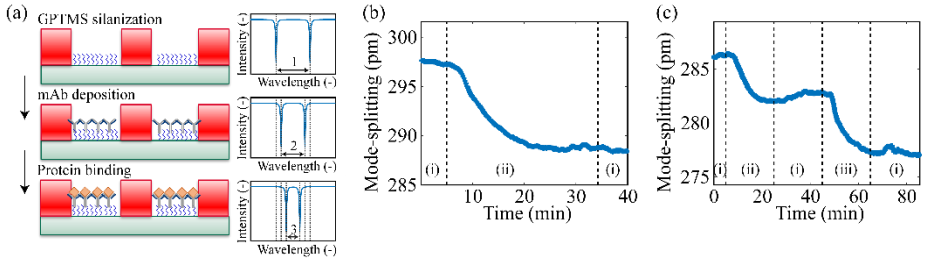

Figure 2. Mode-splitting biosensing. (a) Biomolecule binding to the waveguide surface inside the grating teeth changes the mode-splitting. (b) Change of mode-splitting upon antibodies binding to the grating. (i) 10 mM PBS, (ii) antibodies at a concentration of 200 µg/ml in 10 mM PBS. (c) Change of mode-splitting upon biomarker capture by the antibodies immobilized on the device. (i) 10 mM PBS, (ii) 1 µM rhS100A4 biomarkers in 10 mM PBS, (iii) 5 µM rhS100A4 biomarkers in 10 mM PBS.

4. CONCLUSIONS

This work describes a proof of principle of a self-referenced biosensor using a Bragg grating implemented on a ring resonator. The Bragg grating lifts the degeneracy of the resonator modes resulting in mode-splitting, which depends on the reflectivity of the grating. Since the grating reflectivity only varies very weakly for environmental perturbations such as temperature and bulk refractive index variations, the device can be used as a self-referenced sensor that has almost no response to dielectric perturbations of the bulk medium, whereas it provides a response to structural changes that do affect its reflectivity. Biomolecules were deposited inside the grating teeth, reducing the reflectivity of the grating and hence the amount of mode-splitting, demonstrating the applicability of the device as biosensor.

FUNDING

This work was supported by European Union's Horizon 2020 Framework Programme under grant agreement No 634928 (GLAM). The results presented here reflect only the views of the authors; the European Commission is not responsible for any use that may be made of the information it contains. G.K. receives funding from the Fonds de la Recherche Scientifique -FNRS (Belgium)

REFERENCES

1. A. Mitra, *et al.*, "Nano-optofluidic detection of single viruses and nanoparticles," ACS Nano **4**(3), 1305–1312 (2010).
2. W. Bogaerts, *et al.*, "Silicon microring resonators," Laser Photon. Rev. **27**(1), 47–73 (2011).
3. D. S. Weiss, V. Sandoghdar, J. Hare, V. Lefèvre-Seguin, J.-M. Raimond, and S. Haroche, "Splitting of high-Q Mie modes induced by light backscattering in silica microspheres," Opt. Lett. **20**(18), 1835 (1995).
4. L. He, *et al.*, "Detecting single viruses and nanoparticles using whispering gallery microlasers," Nat. Nanotechnol. **6**(7), 428–432 (2011).
5. L. He, *et al.*, "Scatterer induced mode splitting in poly(dimethylsiloxane) coated microresonators," Appl. Phys. Lett. **96**(22), 2008–2011 (2010).
6. M. de Goede, *et al.*, "Al_2O_3 microring resonators for the detection of a cancer biomarker in undiluted urine," Opt. Express **27**(13), 18508–18521 (2019).
7. B. R. Davies, *et al.*, "Expression of S100A4 protein is associated with metastasis and reduced survival in human bladder cancer," J. Pathol. **196**(3), 292–299 (2002).
8. K. Worhoff, *et al.*, "Reliable Low-Cost Fabrication of Low-Loss Al_2O_3:Er^{3+} Waveguides With 5.4-dB Optical Gain," IEEE J. Quantum Electron. **45**(5–6), 454–461 (2009).
9. J. D. B. Bradley, *et al.*, "Fabrication of low-loss channel waveguides in Al_2O_3 and Y_2O_3 layers by inductively coupled plasma reactive ion etching," Appl. Phys. B **89**(2–3), 311–318 (2007).
10. J. Vörös, "The density and refractive index of adsorbing protein layers," Biophys. J. **87**(1), 553–561 (2004).
11. W. Lee, *et al.*, "Label-Free Prostate Cancer Detection by Characterization of Extracellular Vesicles Using Raman Spectroscopy," Anal. Chem. **90**(19), 11290–11296 (2018).
12. P. Malara, *et al.*, "Fiber Bragg grating laser sensor with direct radio-frequency readout," Opt. Lett. **41**(7), 1420 (2016).
13. N. Acharyya, M. Maher, and G. Kozyreff, "Portable microresonator-based label-free detector: monotonous resonance splitting with particle adsorption," Opt. Express **27**(24), 34997–35011 (2019).